Computational and Theoretical Chemistry 1099 (2017) 174–184

Contents lists available at ScienceDirect

Computational and Theoretical Chemistry

journal homepage: www.elsevier.com/locate/comptc

How the presence of metal atoms and clusters can modify the properties of Silybin? A computational prediction

Miguel Reina, Ana Martínez *

Departamento de Materiales de Baja Dimensionalidad, Instituto de Investigaciones en Materiales, Universidad Nacional Autónoma de México, Circuito Exterior S.N. Ciudad Universitaria, P.O. Box 70-360, Coyoacán C.P. 04510, Ciudad de México, Mexico

ARTICLE INFO

Article history:
Received 31 October 2016
Received in revised form 22 November 2016
Accepted 23 November 2016
Available online 24 November 2016

Keywords:
Donor Acceptor Map
Antioxidants
Metal interaction
Free radicals

ABSTRACT

Silybin and de-protonated silybin are well-known antiradical molecules. The interaction of these two molecules with metal atoms and clusters (tetramers) of Cu, Ag and Au may modify chemical properties. In this report, systems containing metal atoms and clusters (neutral and cationic systems) interacting with silybin and de-protonated silybin are analyzed, by applying Density Functional Theory (DFT) calculations. In order to explore changes in reactivity due to the presence of metals, the free radical scavenging properties of these new systems were studied by analyzing the electron transfer mechanism. Reactivity was also studied by considering the Molecular Electrostatic Potential maps of the most stable systems. Raman spectra were also obtained, both with and without metals. As apparent in this report, electron donor-acceptor capacity is improved with the presence of metals, and the presence of Cu, Ag and Au (atoms and clusters) considerably increases signals from the Raman spectra, which may be useful for experimental detection. The conclusion derived from this study is that the presence of metals not only enhances characterization signals but also modifies electron donor acceptor capacity.

1. Introduction

Silybum marianum (milk thistle) is a medicinal plant that has received tremendous attention during the last decade due to new and emerging applications in medicine and also as a herbal remedy for liver treatment [1–8]. The useful extract from this plant is named silymarin [4], and comprises a natural mixture with beneficial properties for health, specifically related to its hepatoprotective and antiradical characteristics. In previous reports, [9] theoretical studies of the major components of silymarin indicate that, although all components of silymarin have peculiar properties, none of the compounds being studied registered outstanding antiradical capacity compared to the others. In this sense, silymarin is an interesting mixture with antiradical properties and we now know that all components studied present similar chemical properties [9].

The main component of silymarin is silybin (SIL) [3,4]. Silybin is a mixture of two diastereomers: silybin A and silybin B, being silybin B the most abundant in nature. SIL is a molecule with important antiradical properties [9–20]. The antiradical properties of SIL are considered to be responsible for its protective actions. SIL is currently used as an active component in many dietary supplements, cosmetics and dermatological preparations. Studies have also considered the phototoxic potential of the main components of silymarin, however no phototoxicity was revealed for these compounds [21]. It has been suggested that SIL is a potential cancer preventive substance with multifactorial components that manifest anti-cancerogenic activities [22,23]. All these beneficial properties for health are apparently related to its strong antiradical activity. Previous investigations have focused on the antiradical properties of SIL; both theoretical and experimental [24–26]. Electron transfer is one of the reaction mechanisms that is important to analyze. This mechanism measures the capacity of an antiradical molecule to either donate or accept electrons in order to stabilize free radicals.

Antiradical properties of organic molecules change due to the interaction with transition metals [27]. In previous theoretical reports, it was shown that astaxanthin interacts with transition metals such as Cu and Cd [28]. This interaction between astaxanthin and metals modifies antiradical properties and makes the compounds redder in colour. In a subsequent investigation with shrimps, it was demonstrated that shrimps living in water with traces of copper became redder than those living in pure water [29]. Shrimps contain astaxanthin and although it is not possible to say that the change in colour is due to the interaction of astaxanthin and copper, it is a fact that the presence of copper modifies

* Corresponding author.
E-mail address: martina@unam.mx (A. Martínez).

http://dx.doi.org/10.1016/j.comptc.2016.11.030
2210-271X/

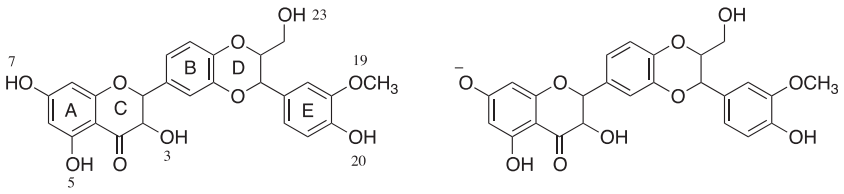

Fig. 1. Silybin (SIL) and de-protonated silybin ($[SIL_{(-H)}]^{-1}$).

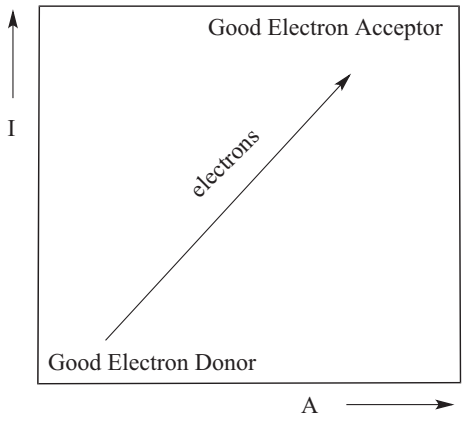

Fig. 2. Full electron donor-acceptor map.

the colour and chemical properties. Astaxanthin's ability to interact with metals is not unique. SIL is capable of interact with transition metals such as Cu^{2+} to produce a complex that has pro-oxidant properties [24–26]. Although all results indicate the antiradical properties of SIL, there are no theoretical investigations that analyze the interaction of SIL with transition metal atoms and clusters. It is however essential to discern how the presence of metal atoms and clusters can modify reactivity, because metals may increase their therapeutic capacity or modify properties so that substances no longer function as possible drugs.

It is well known that the interaction between organic molecules and transition metals increases the possibility of detecting single molecules in solution. Surface-Enhanced Raman Scattering (SERS) [30–32] represents a useful technique resulting in strongly increased Raman signals from molecules, which have been attached to metallic structures. Due to their localized surface plasmon resonance, gold, silver and copper are commonly used to

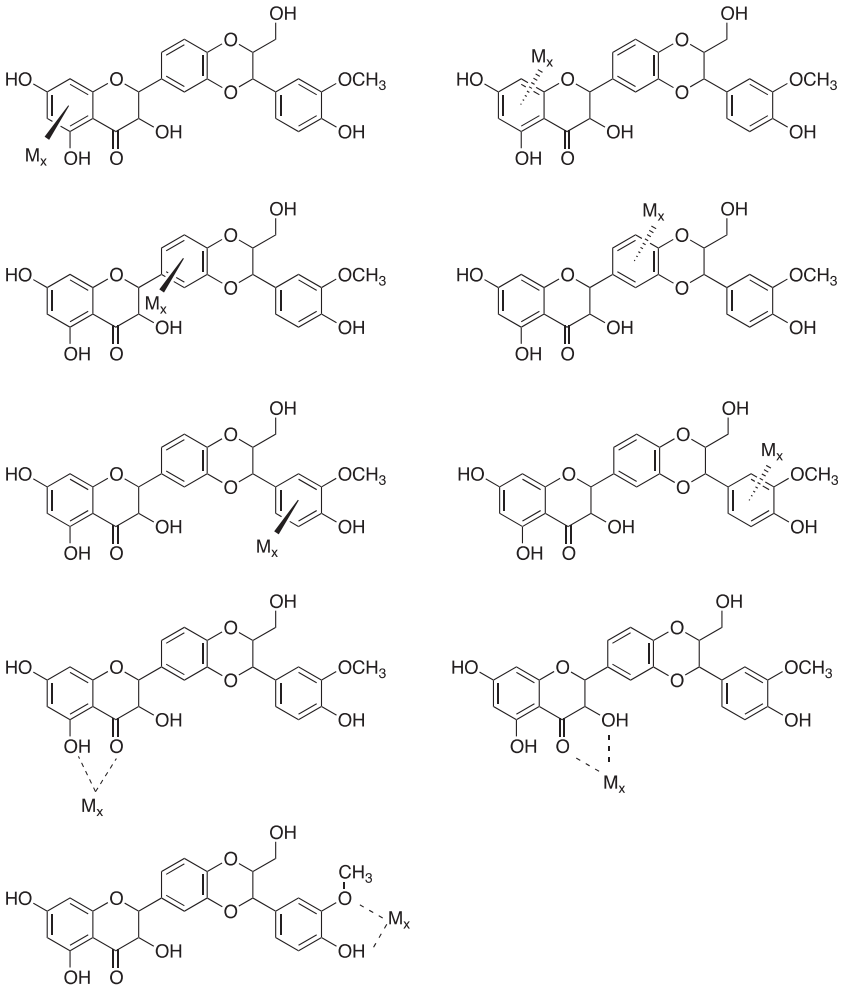

Fig. 3. Schematic representation of the initial geometries for SIL interacting with metal atoms and clusters (neutral and cationic systems). (M is Cu, Ag or Au; x is 1 or 4).

enhance the Raman signals [33]. For SIL, it is important to know if metal atoms and clusters increase the Raman signals in order to give more insights for the experimentalist.

In this report, we investigate the interaction of SIL with copper, silver and gold (atoms and clusters formed with four atoms). We use silybin B since it is 1.99 kcal/mol more stable than silybin A, and the studied properties here are similar for both diastereomers. As it has been demonstrated that under physiological conditions significant amounts of these compounds in their de-protonated form may be present, in this investigation we also consider de-protonated silybin ($[SIL_{(-H)}]^{-1}$). Both SIL and $[SIL_{(-H)}]^{-1}$ are important for explaining the benefits of silymarin. Optimized geometries, Raman spectra and some parameters with which to analyze chemical reactivity are reported for neutral and ionic species. Molecular Electrostatic Potential provides a useful procedure for analyzing charge distribution and inferring chemical reactivity.

2. Computational details

Gaussian 09 implementation [34] was used to calculate geometry optimization and electronic properties of SIL and $[SIL_{(-H)}]^{-1}$ (Fig. 1) interacting with metal atoms and clusters in gas phase. Neutral and cationic species were analyzed. Initial geometries were fully optimized at M06/LANL2DZ level of theory [35–42]. In order to verify optimized minima, harmonic analysis was performed and local minima were identified (zero imaginary frequencies). The lowest spin multiplicity (singlet or doublet) is the most stable for all the systems under study (See Supplementary Material, S13). Theoretical Raman spectra were obtained for all the optimized structures.

To study the interaction between atoms and metal clusters with SIL and $[SIL_{(-H)}]^{-1}$ molecules, the ΔG binding energy was calculated at 298 K, according to the following schemes:

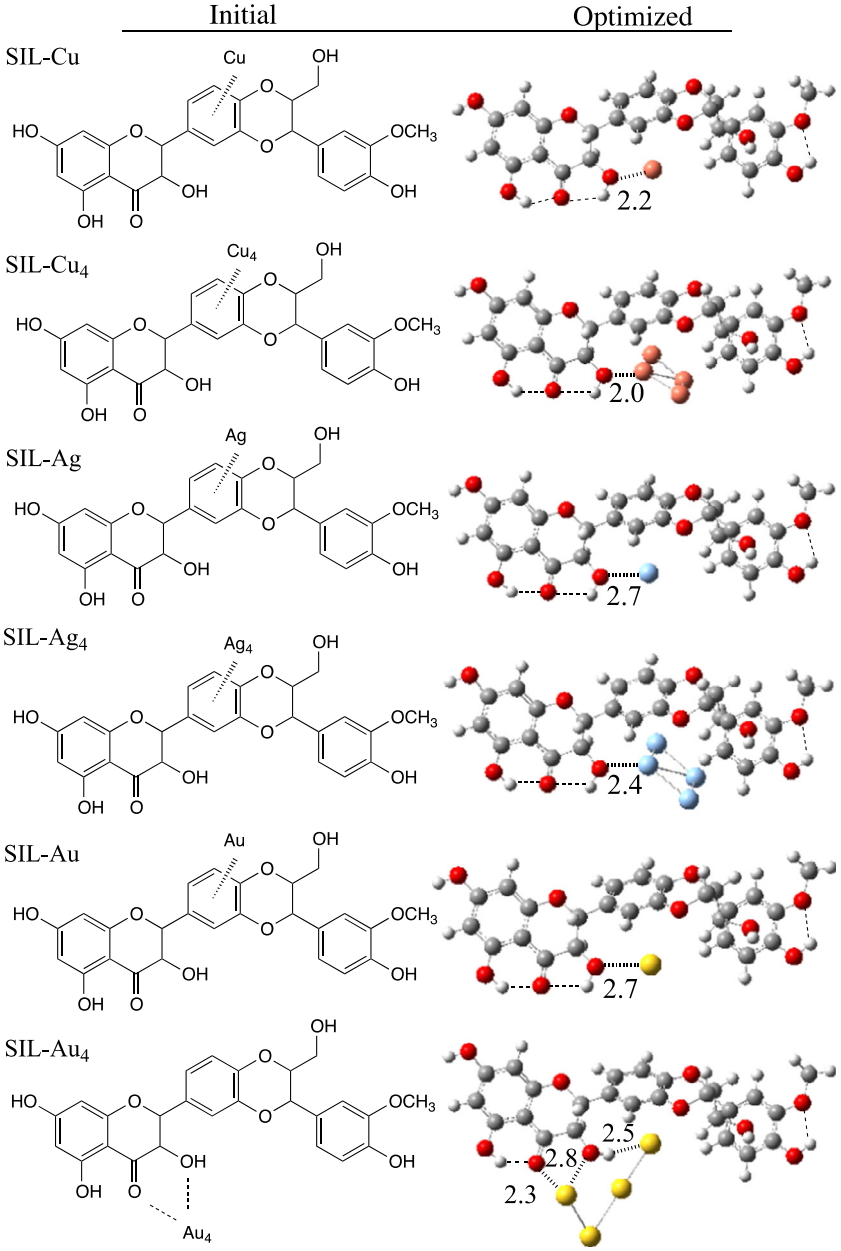

Fig. 4. Schematic and most stable optimized structures of SIL-M_x (M = Cu, Ag or Au; x = 1 or 4).

$$SIL + M_x^q \rightarrow SIL\text{-}M_x^q \quad (1)$$

$$[SIL_{(-H)}]^{-1} + M_x^q \rightarrow [SIL_{(-H)}\text{-}Mx]^{q-1} \quad (2)$$

SIL and $[SIL_{(-H)}]^{-1}$ are the two organic molecules under study, M is Cu, Ag or Au, x is the number or metal atoms (1 or 4), q symbolizes the atomic or molecular charge (0 or +1) and $SIL\text{-}M_x^q$ and $[SIL_{(-H)}\text{-}Mx]^{q-1}$ represents the metal atoms and clusters interacting with SIL and $[SIL_{(-H)}]^{-1}$. ΔG binding energy is as follows:

$$\Delta G = G(SIL\text{-}M_x^q) - [G(SIL) + G(M_x^q)] \quad (3)$$

$$\Delta G = G\left([SIL_{(-H)} - M_x]^{q-1}\right) - \left[G\left([SIL_{(-H)}]^{-1}\right) + G(M_x^q)\right] \quad (4)$$

In order to investigate the single electron transfer mechanism, vertical ionization energy (I) and vertical electron affinity (A) were obtained from single point calculations of cationic and anionic molecules, using the optimized structure of the neutrals and the 6-311+g(d,p) basis set for C, H and O and LANL2DZ for metal atoms. Water was included to simulate polar environment with SMD continuum model [43]. A useful tool defined previously is the electron Full Electron Donor Acceptor Map (FEDAM) [44,45]. In this map (see Fig. 2) I and A are plotted and allow us to classify substances as either donors or acceptors of electrons. Electrons will be transferred from molecules located down to the left of the map (good electron donors) to those molecules that are up to the right (good electron acceptors).

The Molecular Electrostatic Potential of a molecule is a good guide to assess the reactivity towards reactants positively or negatively charged and furthermore to analyze changes in charge distribution. Molecular Electrostatic Potential was obtained for SIL and $[SIL_{(-H)}]^{-1}$ and the new systems formed, $SIL\text{-}M_x^q$ and $[SIL_{(-H)}\text{-}M_x]^{q-1}$, using the total electron density to analyze the force acting on a positive test charge located in the vicinity of a

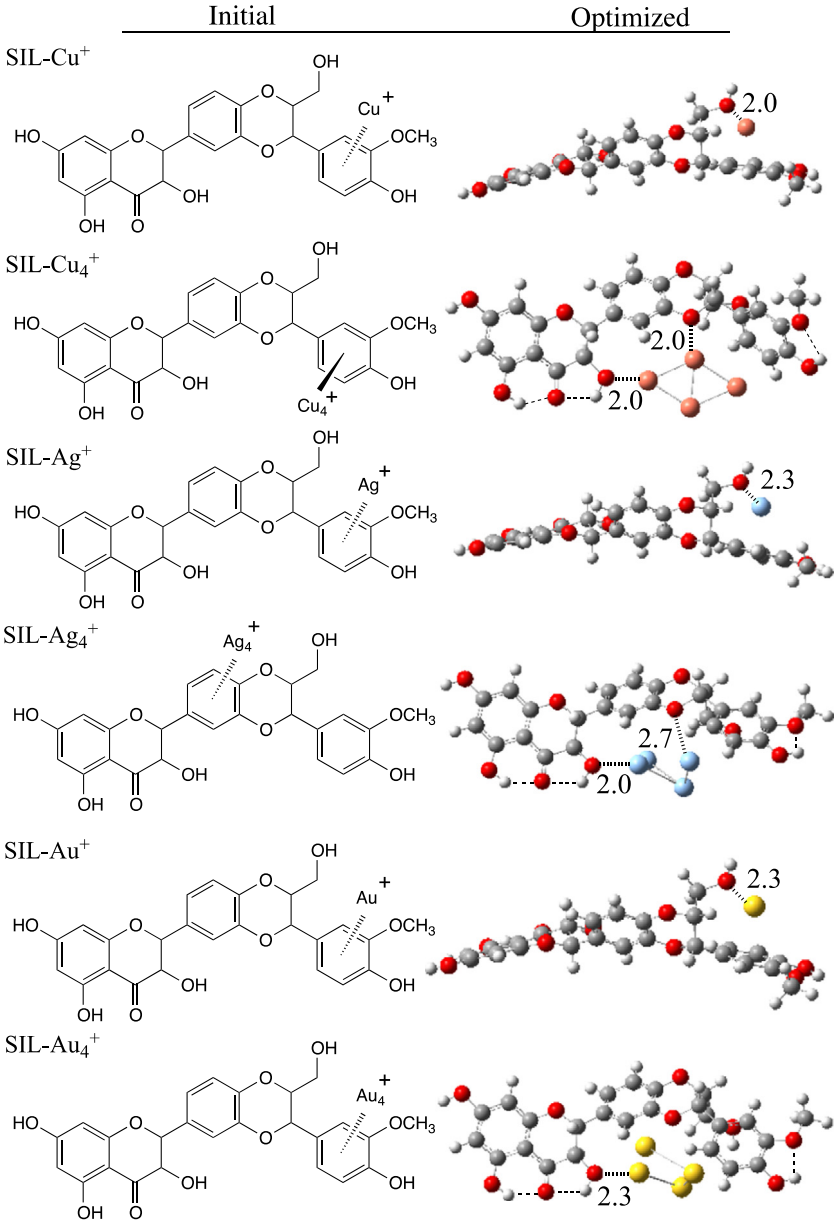

Fig. 5. Schematic initial structure and most stable optimized structures of $[SIL\text{-}M_x]^+$ (M = Cu, Ag and Au; x = 1 or 4).

molecule. It is important to note that no polarization of the molecule occurs and therefore, the molecular charge distribution remains unperturbed through the external test charge. Red colour of the Molecular Electrostatic Potential is the negative section of the molecule and the blue one is positive (low electron density).

3. Results and discussion

3.1. Geometry optimization

Several initial geometries were used to analyze the ground state structures of metal atoms and clusters interacting with SIL. Fig. 3 reports the schematic representation of the initial geometries for SIL interacting with metal atoms and clusters (neutral and cationic systems). The main reason for studying the interaction of SIL with a single metal atom is to investigate whether this atom modifies the Raman spectra and how the free radical scavenging properties of SIL change due to the presence of metals. We also include the tetramer because there are studies that define Ag_4 as the minimum cluster size for producing the latent image of a picture, [46] when $AgNO_3$ was used in photography. Apparently, four is the minimum number of metal atoms in a metal cluster that are able to modify physicochemical properties in an interesting way.

In Fig. 4, the most stable optimized structures for SIL and SIL-M_x are reported. For each ground state, we include the schematic representation of the initial geometry. During optimization, metal atoms and clusters do not always remain at the same initial position. There are other optimized structures that have similar stability (see Supplementary Material). The energy difference between the most stable structures and the next ones is less than 5 kcal/mol in some cases. Apparently, the position of the metal atoms or clusters around the SIL molecule does not modify stability. As structures with similar stability have similar properties, in the following we will focus on the most stable structures.

In Fig. 4, the most stable optimized structures are similar for systems with one metal atom. M is bonded to the same oxygen atom of SIL, and as expected Cu—O bond distance is slightly shorter than Ag—O and Au—O bond length. The most stable SIL-M compounds show the three intramolecular hydrogen bonds of SIL. For SIL-Cu, SIL-Ag and SIL-Au, there are other structures that are very close to the ground state system (reported in Supplementary Material). The energy difference between these structures is less than 5 kcal/mol so they could coexist in an experiment.

The structures of SIL-Cu_4 and SIL-Ag_4 are similar. The ground state has C—M and O—M bonds, and SIL has three intramolecular hydrogen bonds. Both stable structures have one metal atom bonded to O(3) (see Fig. 1). SIL-Au_4 deserves special attention as the most stable structure presents one gold atom forming a non-conventional hydrogen bond, and SIL has two intramolecular hydrogen bonds instead of three. Non-conventional hydrogen bonds were previously reported for gold systems and it is already known that they stabilize systems [47,48]. The H—Au bond length is 2.5 Å. There is also a bond between Au and two oxygen atoms of SIL that makes the system more stable. This is the only SIL-Au_4 structure that shows non-conventional hydrogen bonds. Comparing this structure with those that are less stable (not shown in the figure, see Supplementary Material), it is possible to see that this non-conventional hydrogen bond stabilizes the system by 2.5 kcal/mol.

The cations were also optimized in order to investigate the influence of the charge. Fig. 5 reports the most stable optimized structures for $[SIL\text{-}M_x]^{+1}$ (M = Cu, Ag or Au; x = 1 or 4) and the corresponding schematic structures of the initial geometries. In Fig. 5, it is evident that the most stable structures of $[SIL\text{-}M_x]^{+1}$ are those where a metal atom is bonded to O(23) (see Fig. 1). [SIL—M]$^+$ bond lengths are shorter than SIL—M bond distances and as expected, Cu—O length is shorter than Ag—O and Au—O bond distances. The cationic structures present much larger differences in energy values between the most stable compound and the second one (Supplementary Material). Analyzing the cationic systems with clusters, structures with metal atoms bonded to oxygen atoms of SIL are the most stable systems. Fig. 5 shows all structures with three intramolecular hydrogen bonds of SIL. For the $[SIL\text{-}Ag_4]^+$ and $[SIL\text{-}Au_4]^+$ structures, clusters are no longer planar but tetrahedral, whereas in $[SIL\text{-}Cu_4]^+$ the cluster remains planar.

As already explained in the introduction, a considerable amount of de-protonated silybin ($[SIL_{(-H)}]^{-1}$) exists under physiological conditions. SIL is used for the treatment of diseases under physiological conditions and therefore it may be that both molecules have an effect. For this reason, the investigation of $[SIL_{(-H)}]^{-1}$ interacting with metal atoms and clusters is important. In order to define initial geometries, the Molecular Electrostatic Potential of $[SIL_{(-H)}]^{-1}$ was analyzed and is shown in Fig. 6.

As anticipated, in Fig. 6 the negative region of the molecule (red colour) is close to the de-protonated oxygen atom. It is clear that the interaction with metal atoms and clusters, neutrals and cations, will most probably be with this oxygen atom. We tested other initial geometries but they optimized to less stable structures and are thus not included in this report. The most stable optimized structures for $[SIL_{(-H)}]^{-1}$ interacting with metal atoms and clusters (neutral and cations) are reported in Fig. 7. In Fig. 7, the terms "anionic" and "neutral" corresponds to the charge of the system.

These optimized structures present the same M—O bond. The bond distances are shorter for the cations than for the neutrals in all systems, and in all the optimized structures, the three intramolecular hydrogen bonds of $[SIL_{(-H)}]^{-1}$ remain. Slight deformations of clusters can also be observed but they are all planar structures.

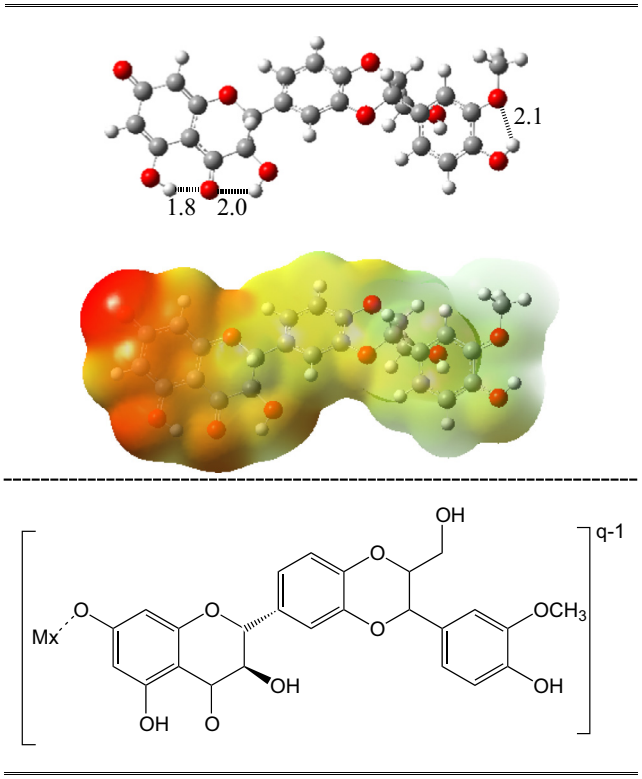

Fig. 6. Most stable structure of $[SIL_{(-H)}]^{-1}$ and its Molecular Electrostatic Position are reported. Schematic representation of the initial geometry for $[SIL_{(-H)}\text{-}M_x]^{q-1}$ (M = Cu, Ag or Au; x = 1 or 4; q = 0 or 1) is also included.

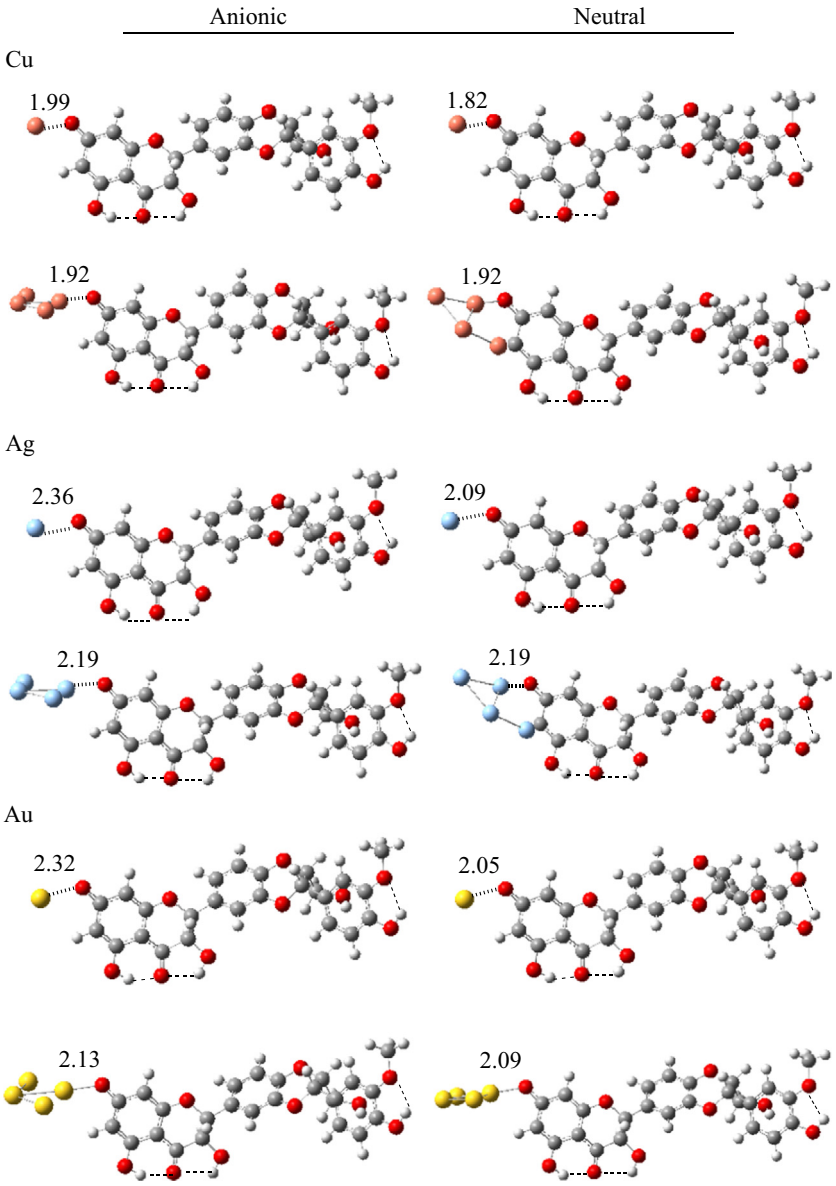

Fig. 7. Most stable structures of $[SIL_{(-H)}\text{-}M_x]^{q-1}$ (M = Cu, Ag or Au; x = 1 or 4; q = 0 or 1).

ΔG binding energies for all systems are reported in Table 1. All SIL reactions with metal atoms and clusters are exergonic, and the reaction with clusters is more exergonic than that with atoms. Comparing SIL with $[SIL_{(-H)}]^{-1}$, the latter are more exergonic than the former and the interactions between charged species are more spontaneous. Cu systems present more negative values than Ag and Au in all systems and therefore the reaction is more spontaneous with this metal.

3.2. Raman spectra

The detection of small amounts of these substances is important when they are used therapeutically. It has already been demonstrated that the presence of metals may increase the signals of the spectra [49]. Following this idea, Raman spectra for the most stable structures are shown in Figs. 8 and 9, and the main signals are reported in Tables 2 and 3, for SIL and $[SIL_{(-H)}]^{-1}$, respectively. In each spectrum, typical signals for each system are indicated with a star and Tables 2 and 3 summarize the main differences. With one metal atom interacting with SIL, a difference is already apparent. The spectra of SIL and $[SIL_{(-H)}]^{-1}$ are less intense than the spectra with metal atoms. A single metal atom produces signals that are not present when metals are absent. There is a signal

Table 1
Bonding energies ΔG (kcal/mol) for the following scheme reactions: $M_x^q + SIL \rightarrow SIL\text{-}M_x^q$ and $M_x^q + [SIL_{(-H)}]^{-1} \rightarrow [SIL_{(-H)}\text{-}Mx]^{q-1}$ (M is Cu, Ag or Au, x is 1 or 4 and q is 0 or +1).

Molecule	ΔG (kcal/mol)	Molecule	ΔG (kcal/mol)
SIL-Cu	−7.4	$[SIL_{(-H)}\text{-}Cu]^{-1}$	−15.7
$SIL\text{-}Cu^+$	−81.8	$[SIL_{(-H)}\text{-}Cu]^{0}$	−148.2
$SIL\text{-}Cu_4$	−20.7	$[SIL_{(-H)}\text{-}Cu_4]^{-1}$	−31.1
$SIL\text{-}Cu_4^+$	−52.6	$[SIL_{(-H)}\text{-}Cu_4]^{0}$	−124.7
SIL-Ag	−2.8	$[SIL_{(-H)}\text{-}Ag]^{-1}$	−8.0
$SIL\text{-}Ag^+$	−54.4	$[SIL_{(-H)}\text{-}Ag]^{0}$	−124.8
$SIL\text{-}Ag_4$	−11.9	$[SIL_{(-H)}\text{-}Ag_4]^{-1}$	−22.6
$SIL\text{-}Ag_4^+$	−34.2	$[SIL_{(-H)}\text{-}Ag_4]^{0}$	−103.5
SIL-Au	−2.7	$[SIL_{(-H)}\text{-}Au]^{-1}$	−10.8
$SIL\text{-}Au^+$	−71.0	$[SIL_{(-H)}\text{-}Au]^{0}$	−146.4
$SIL\text{-}Au_4$	−18.3	$[SIL_{(-H)}\text{-}Au_4]^{-1}$	−30.2
$SIL\text{-}Au_4^+$	−47.9	$[SIL_{(-H)}\text{-}Au_4]^{0}$	−113.5

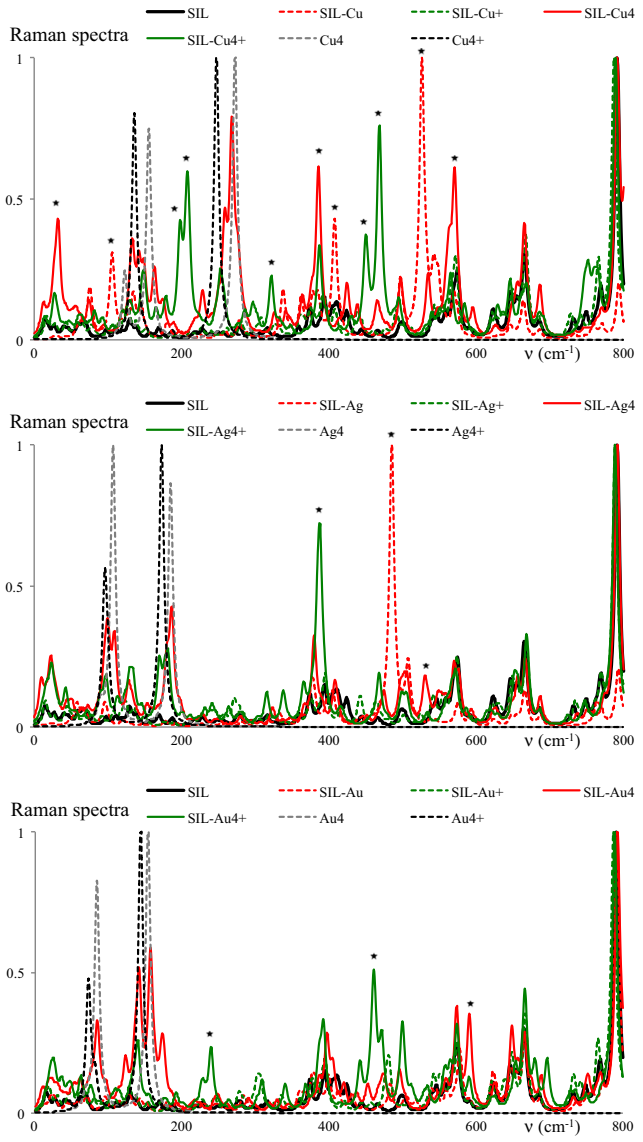

Fig. 8. Raman spectra of SIL-M_x and SIL-M_x^{+1} (M = Cu, Ag or Au; x = 1 or 4). The main different data are also included.

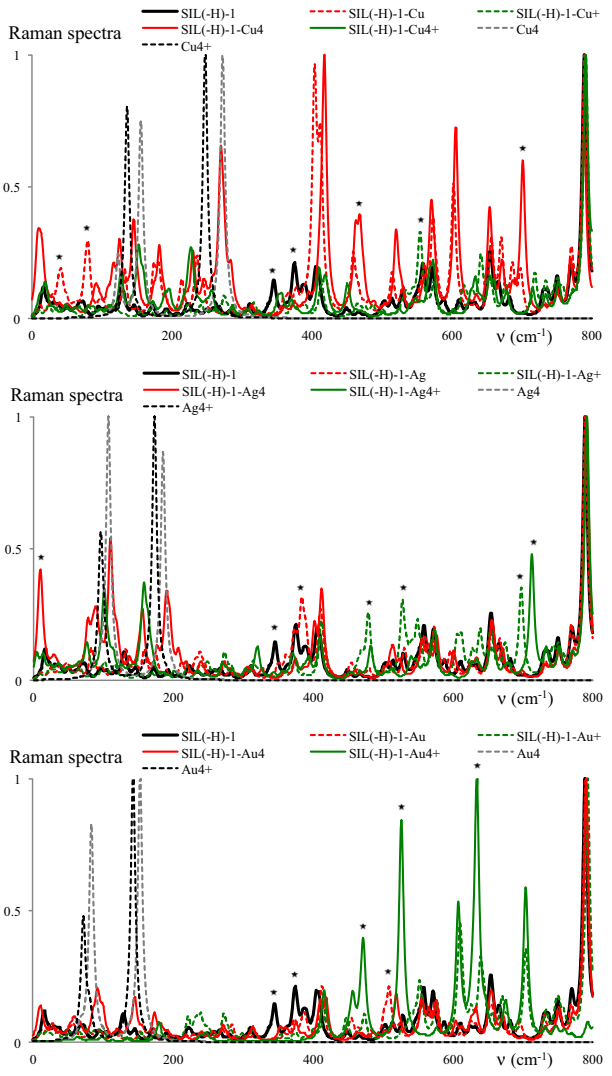

Fig. 9. Raman spectra of $[SIL_{(-H)}]^{-1}$ and $[SIL_{(-H)}\text{-}M_x]^{q-1}$ (M = Cu, Ag or Au; x = 1 or 4; q = 0 or 1). The main different data are also included.

at 343 cm^{-1} for $[SIL_{(-H)}]^{-1}$ that disappears when metal atoms and clusters are present. Other differences of the spectra due to the presence of metal clusters are indicated in the figures.

If we compare the systems with Cu, Ag and Au, it is evident that all metals produce more or less the same effects. An increment in signals due to the presence of the metals occurs in all systems, and there are some peaks that are typical. Therefore, it is possible to conclude that this is useful for detecting the existence of metals. These results are crucial, as they indicate that the presence of a very small concentration of metals may increase the signals in such a way that detection is more precise and sensitive.

3.3. Electron transfer mechanism

Figs. 10 and 11 report the FEDAM for the systems with metal atoms and with metal clusters, respectively. Three free radicals ($^{\cdot}OOH$, $NO_2^{\cdot}$, $DPPH^{\cdot}$) are included for comparison. The electrons will be transferred from the systems located down to the left to those placed up to the right. In general, the presence of metals (atoms and clusters) produces changes in *I* and *A*. *I* decreases in most cases, making these systems better electron donors than SIL or $[SIL_{(-H)}]^{-1}$.

Table 2
Main Raman spectra signals of SIL-M_x and SIL-M_x^{+1} (M = Cu, Ag or Au; x = 1 or 4).

System	ν (cm^{-1})
SIL	Less intense spectrum
SIL-Cu_x^q	
SIL-Cu	105, 407, 526
SIL-Cu^+	–
SIL-Cu_4	31, 385, 570
SIL-Cu_4^+	197, 207, 320, 449, 468
Cu_4 and Cu_4^+	All important signals smaller than 300 cm^{-1}
SIL-Ag_x^q	
SIL-Ag	485
SIL-Ag^+	–
SIL-Ag_4	528
SIL-Ag_4^+	386
Ag_4 and Ag_4^+	All important signals smaller than 200 cm^{-1}
SIL-Au_x^q	
SIL-Au	–
SIL-Au^+	–
SIL-Au_4	590
SIL-Au_4^+	238, 460
Au_4 and Au_4^+	All important signals smaller than 200 cm^{-1}

Table 3
Main Raman spectra signals of $[SIL_{(-H)}]^{-1}$ and $[SIL_{(-H)}\text{-}M_x]^{q-1}$ (M = Cu, Ag or Au; x = 1 or 4; q = 0 or 1).

System	ν (cm^{-1})
$[SIL_{(-H)}]^{-1}$	Less intense spectrum, 343, 373
$[SIL_{(-H)}\text{-}Cu_x]^q$	
$[SIL_{(-H)}\text{-}Cu]^{-1}$	38, 77
$[SIL_{(-H)}\text{-}Cu]^0$	553
$[SIL_{(-H)}\text{-}Cu_4]^{-1}$	462, 701
$[SIL_{(-H)}\text{-}Cu_4]^0$	–
Cu_4 and Cu_4^+	All important signals smaller than 300 cm^{-1}
$[SIL_{(-H)}\text{-}Ag_x]^q$	
$[SIL_{(-H)}\text{-}Ag]^{-1}$	382
$[SIL_{(-H)}\text{-}Ag]^0$	478, 527, 697
$[SIL_{(-H)}\text{-}Ag_4]^{-1}$	9
$[SIL_{(-H)}\text{-}Ag_4]^0$	712
Ag_4 and Ag_4^+	All important signals smaller than 200 cm^{-1}
$[SIL_{(-H)}\text{-}Au_x]^q$	
$[SIL_{(-H)}\text{-}Au]^{-1}$	519
$[SIL_{(-H)}\text{-}Au]^0$	–
$[SIL_{(-H)}\text{-}Au_4]^{-1}$	–
$[SIL_{(-H)}\text{-}Au_4]^0$	471, 526, 634
Au_4 and Au_4^+	All important signals smaller than 200 cm^{-1}

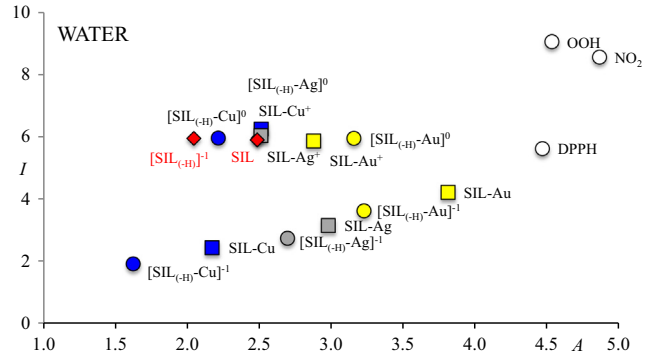

Fig. 10. FEDAM for SIL, $[SIL_{(-H)}]^{-1}$, $[SIL\text{-}M]^q$ and $[SIL_{(-H)}\text{-}M]^{q-1}$ (M = Cu, Ag or Au; q = 0 or 1). Free radicals are included for comparison.

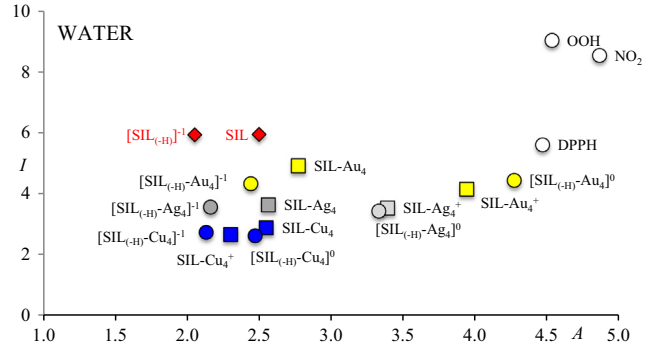

Fig. 11. FEDAM for SIL, $[SIL_{(-H)}]^{-1}$, $[SIL\text{-}M_4]^q$ and $[SIL_{(-H)}\text{-}M_4]^{q-1}$ (M = Cu, Ag or Au; q = 0 or 1). Free radicals are included for comparison.

Electron acceptor capacity is increased in some cases (*A* is larger than for SIL or $[SIL_{(-H)}]^{-1}$) but this is not a general pattern. Notably, the presence of only one metal atom modifies electron donor acceptor capacity and thus the reactivity of the systems. Two free radicals, ·OOH and $NO_2^{\cdot}$ are the best electron acceptors. To scavenge these free radicals, the systems must be good electron donors. DPPH· is also a good electron acceptor and all good electron donors are able to scavenge this free radical. The best electron donor systems are compounds of SIL and $[SIL_{(-H)}]^{-1}$ with Cu (atom and cluster); thus these are the best free radical scavenger molecules. The best electron acceptors are systems with Au, which are thus the best free radical scavenger molecules for free radicals that accept electrons such as O_2^- (not shown in figure, see Ref. [50]). In summary, the presence of metals (atoms and clusters) modifies the electron transfer capacity of SIL and $[SIL_{(-H)}]^{-1}$. This may constitute an advantage for therapeutic purposes, but it is clear that further research is necessary. The therapeutic properties of these molecules may be related to their electron transfer properties, as the electron transfer represents one of the antiradical (or free radical scavenger) mechanisms. If this is so, then the metal atoms and clusters may produce an increment in the protective actions of SIL and $[SIL_{(-H)}]^{-1}$. More studies about the relationship between the electron transfer capacity and the therapeutic efficiency of SIL or $[SIL_{(-H)}]^{-1}$ interacting with metal atoms and clusters are necessary.

3.4. Molecular electrostatic potential

Molecular Electrostatic Potential enables us to analyze the regions of the molecules that are positively (blue) or negatively (red) charged and therefore more susceptible to nucleophilic or electrophilic additions. Figs. 12 and 13 present the Molecular Electrostatic Potential for Cu_4 interacting with SIL and $[SIL_{(-H)}]^{-1}$. Results with other metals and clusters are not included as they are similar. Comparing the Molecular Electrostatic Potential for the neutral systems, it is possible to see that they are very similar to the Molecular Electrostatic Potential of the SIL (Fig. 12 two first structures). The presence of Cu_4 does not alter the charge distribution of the molecule and the same reactivity can be expected. However, the presence of the cationic clusters modifies the Molecular Electrostatic Potential of SIL (Fig. 12, third structure). The positive section of the molecule is located close to the cationic cluster. Therefore, reactivity could be different. Similar charge distribution is found with $[SIL_{(-H)}\text{-}Cu_4]^0$ (Fig. 13, third structure) The positive charge is located on the cluster and the negative section is less negative in comparison with $[SIL_{(-H)}]^{-1}$. The presence of the cationic cluster modifies the charge distribution all over the molecule and this may alter not only reactivity, but also biological activity.

4. Concluding remarks

The most stable Cu, Ag and Au structures of atoms and metallic clusters interacting with SIL and $[SIL_{(-H)}]^{-1}$ are presented. ΔG binding energies show that all systems are thermodynamically spontaneous, and in this way charged systems are more favourable than neutral systems. The Raman spectra are useful for identifying the different systems, as the presence of metal atoms and clusters produce substantial changes, enhancing signals of the SIL and $[SIL_{(-H)}]^{-1}$ spectra. Almost every system has typical signals in the Raman spectra, making characterization possible. Moreover, it is feasible to distinguish between SIL and $[SIL_{(-H)}]^{-1}$.

The electron transfer mechanism is important for scavenging free radicals. The presence of metals increases the electron transfer capacity of SIL and $[SIL_{(-H)}]^{-1}$, also increasing antiradical capability. SIL and $[SIL_{(-H)}]^{-1}$ scavenge free radicals but the compounds formed with SIL or $[SIL_{(-H)}]^{-1}$ and metals are better electron donor-acceptor compounds and therefore, better free radical scavengers.

The Molecular Electrostatic Potential of SIL and $[SIL_{(-H)}]^{-1}$ are not altered by the presence of neutral clusters, but the interactions with cationic clusters modify charge distribution and probably reactivity. This may be important for therapeutic purposes. Further research is required to discern whether or not SIL and $[SIL_{(-H)}]^{-1}$

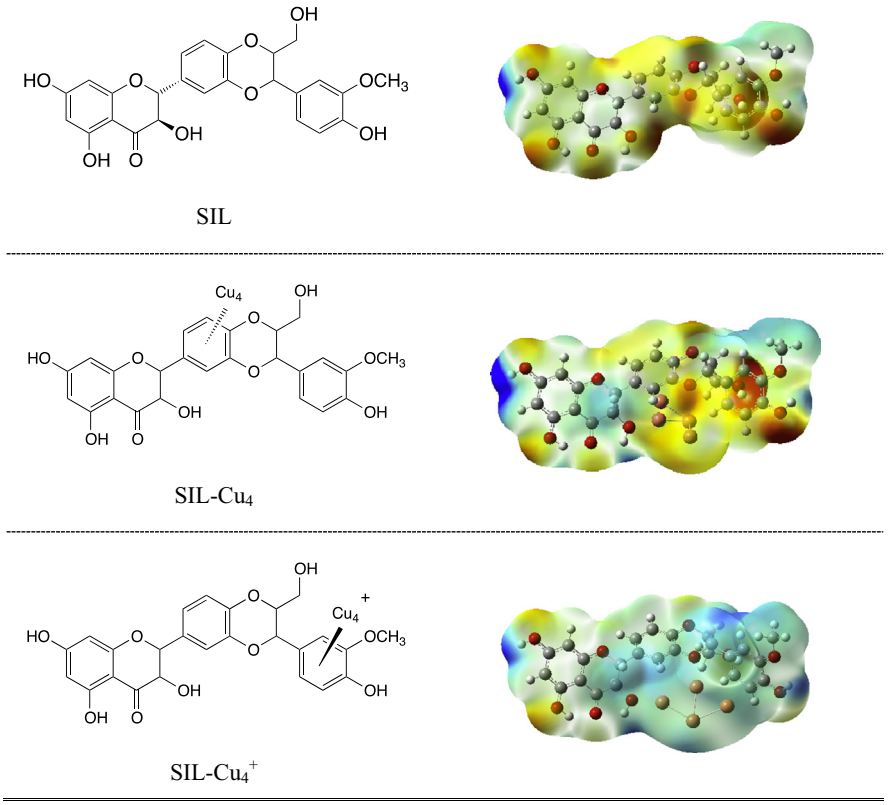

Fig. 12. SIL, SIL-Cu_4 and SIL-Cu_4^+: schematic representation of the structure and Molecular Electrostatic Potential.

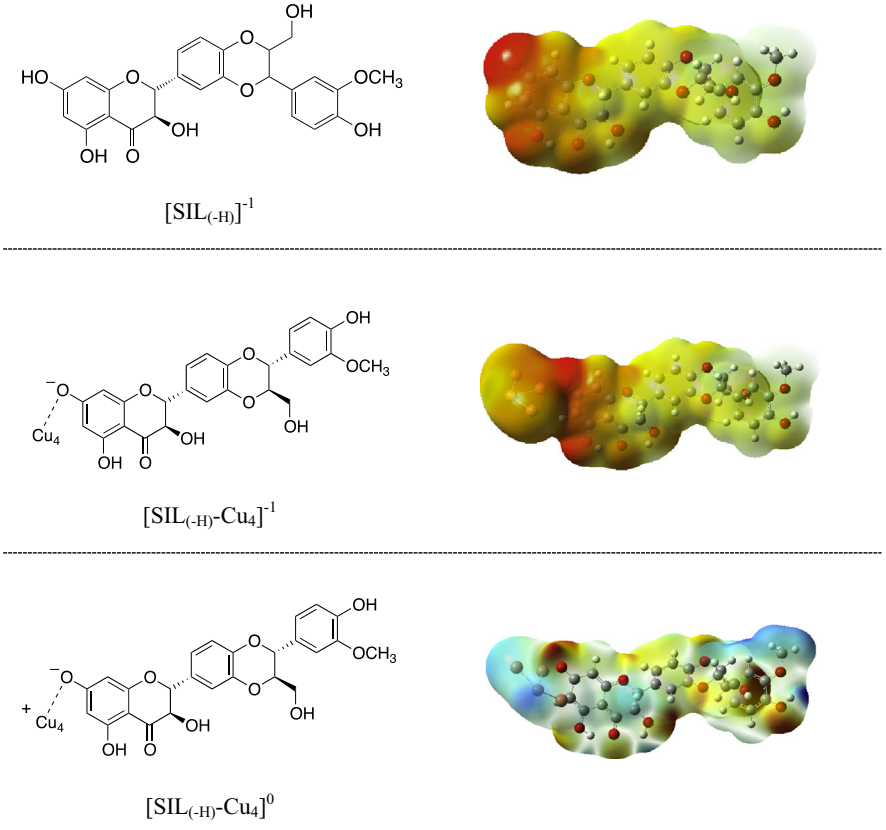

Fig. 13. Schematic representation of the structure and Molecular Electrostatic Potential.

interacting with metal atoms and clusters manifest properties that are appropriate for therapeutic procedures.

Acknowledgements

This study was funded by DGAPA-PAPIIT, Consejo Nacional de Ciencia y Tecnología (CONACyT), and resources provided by the Instituto de Investigaciones en Materiales (IIM). This work was carried out using a NES supercomputer, provided by Dirección General de Cómputo y Tecnologías de Información y Comunicación (DGTIC), Universidad Nacional Autónoma de México (UNAM). We would like to thank the DGTIC of UNAM for their excellent and free supercomputing services and Caroline Karslake (Masters, Social Anthropology, Cambridge University, England) for reviewing the grammar and style of the text in English. The authors would like to acknowledge Oralia L Jiménez A., María Teresa Vázquez and Caín González for their technical support. MR thanks CONACyT for the PhD scholarship (387687).

This research did not receive any specific grant from funding agencies in the public, commercial, or not-for profit sectors.

Appendix A. Supplementary material

Supplementary data associated with this article can be found, in the online version, at http://dx.doi.org/10.1016/j.comptc.2016.11.030.

References

[1] P. Morazzoni, E. Bombardelli, *Silybum marianum* (*Carduus marianus*), Fitoterapia LXVI (1995) 3–42.
[2] D. Schuppan, J.D. Jia, B. Brinkhaus, E.G. Hahn, Herbal products for liver diseases: a therapeutic challenge for the new millennium, Hepatology 30 (1999) 1099–1104.
[3] V. Šimánek, V. Křen, J. Ulrichová, J. Vicar, L. Cvak, Silymarin: what is in the name...? An appeal for a change of editorial policy, Hepatology 32 (2000) 442–444.
[4] H. Wagner, L. Hörhammer, R. Münster, On the chemistry of silymarin (silybin), the active principle of the fruits of *Silybum marianumv*(*L*) Gaertn. (*Carduus marianus L.*), Arzneimittelforschung 18 (1968) 688–696.
[5] R. Gažák, D. Walterová, V. Křen, Silybin and silymarin-new and emerging applications in medicine, Curr. Med. Chem. 14 (2007) 315.
[6] R. Saller, R. Meier, R. Brignoli, The use of silymarin in the treatment of liver diseases, Drugs 61 (2001) 2035–2063.
[7] K. Wellington, B. Jarvis, Silymarin: a review of its clinical properties in the management of hepatic disorders, BioDrugs 15 (2001) 465–489.
[8] S. Balian, S. Ahmad, R. Zafar, Antiinflammatory activity of leaf and leaf callus of *Silybum marianum* (*L.*) *Gaertn.* in albino rats. Indian, J. Pharmacol. 38 (2006) 213–214.
[9] M. Reina, A. Martínez, Is silybin the best free radical scavenger compound in silymarin?, J Phys. Chem. B 120 (2016) 4568–4579.
[10] C. Loguercio, D. Festi, Silybin and the liver: from basic research to clinical practice, World J. Gastroenterol. 17 (2011) 2288–2301.
[11] P.F. Surai, Silymarin as a natural antioxidant: an overview of the current evidence and perspectives, Antioxidants 4 (2015) 204–247.
[12] L. Mira, M. Silva, C.F. Manso, Scavenging of reactive oxygen species by silybin dihemisuccinate, Biochem. Pharmacol. 48 (1994) 753–759.
[13] R. Gazák, A. Svobodová, J. Psotová, P. Sedmera, V. Prikrylová, D. Walterová, V. Kren, Oxidised derivatives of silybin and their antiradical and antioxidant activity, Bioorg. Med. Chem. 12 (2004) 5677–5687.
[14] A. Jain, N. Dwivedi, R. Bhargava, S.J.S. Flora, Silymarin and naringenin protects nicotine induced oxidative stress in young rats, Oxidants Antioxidants Med. Sci. 1 (2012) 41–49.
[15] I. György, S. Antus, A. Blázovics, G. Földiák, Substituent effects in the free radical reactions of silybin: radiation-induced oxidation of the flavonoid at neutral pH, Int. J. Rad. Biol. 61 (1992) 603–609.
[16] E. van Wenum, R. Jurczakowski, G. Litwinienki, Media effects on the mechanism of antioxidant action of silybin and 2,3-dehydrosilybin: role of the enol groups, J. Org. Chem. 78 (2013) 9102–9112.
[17] K. Lemaska, H. Szymusiak, B. Tyrakowska, T. Zieliski, A.E.M. Soffers, I.M.C. Rietjens, The influence of pH on antioxidant properties and the mechanism of antioxidant action of hydroxylflavones, Free Rad. Biol. Med. 31 (2001) 869–881.
[18] P. Trouillas, P. Marsal, A. Svobodová, J. Vostálová, R. Gazak, J. Hrbác, P. Sedmera, V. Kren, R. Lazzaroni, J.L. Duroux, D. Walterová, Mechanism of the antioxidant action of silybin and 2,3-dehydrosilybin flavonolignans: a joint experimental and theoretical study, J. Phys. Chem. A 112 (2008) 1054–1063.
[19] M. Reina, A. Martínez, Silybin and 2,3-dehydrosilybin flavonolignans as free radical scavengers, J. Phys. Chem. B 119 (2015) 11597–11606.
[20] S. Fan, M. Qi, Y. Yu, L. Li, G. Yao, S. Tashiro, S. Onodera, T. Ikejima, P53 activation plays a crucial role in silibinin induced ROS generation via PUMA and JNK, Free Radic Res. 46 (2012) 310–319.
[21] A. Rajnochová, A. Svobodová, B. Zálešák, D. Biedermann, J. Ulrichová, J. Vostálová, Phototoxic potential of silymarin and its bioactive components, J. Photochem. Photobiol. B: Biol. 156 (2016) 61–68.
[22] R. Agarwal, C. Agarwal, H. Ichikawa, R.P. Singh, B.H. Aggarwal, Anticancer potential of silymarin: from bench to bed side, Antican. Res. 26 (2006) 4457–4498.
[23] S.K. Katiyar, Silymarin and skin cancer prevention: anti-inflammatory, antioxidant and immunomodulatory effects, Int. J. Oncol. 26 (2005) 169.
[24] M. Zatloukalová, V. Křen, R. Gažák, M. Kubala, P. Trouillas, J. Ulrichová, J. Vacek, Electrochemical investigation of flavonolignans and study of their interactions with DNA in the presence of Cu(II), Bioelectrochemistry 82 (2011) 117–1124.
[25] M. Borsari, C. Gabbi, F. Ghelfi, R. Grandi, M. Saladini, S. Sverei, F. Borella, Silybin, a new iron-chelating agent, J. Inor. Biochem. 85 (2001) 123–129.
[26] M. Gharagozloo, Z. Khoshdel, Z. Amirghofran, The effect of an iron (III) chelator, silybin, on the proliferation and cell cycle of Jurkat cells: a comparison with desferrioxamine, Eur. J. Pharmacol. 589 (2008) 1–7.
[27] A. Galano, G. Mazzone, R. Álvarez-Diduk, T. Marino, J.R. Álvarez-Idaboy, N. Russo, Food antioxidants: chemical insights at the molecular level, Annu. Rev. Food Sci. Technol. 7 (2016) 335–352.
[28] E. Hernández-Marín, A. Barbosa, A. Martínez, The metal cation chelating capacity of astaxanthin. Does this have any influence on antiradical capacity?, Molecules 17 (2012) 1039–1054
[29] A. Martínez, Y. Romero, T. Castillo, M. Mascaró, I. López-Rull, N. Simões, F. Arcega-Cabrera, G. Gaxiola, A. Barbosa, The effect of copper on the color of shrimps:redder is not always healthier, PLoS ONE 9 (2014) e107673.
[30] K. Kneipp, Y. Wang, H. Kneipp, L.T. Perlman, I. Itzkan, R.R. Dasari, M.S. Feld, Single molecule detection using surface-enhanced Raman scattering (SERS), Phys. Rev. Lett. 78 (1997) 1667–1679.
[31] E.C. Le Ru, E. Blackie, M. Meyer, P.G. Etchegoin, Surface enhanced Raman scattering enhancement factors: a comprehensive study, Phys. Chem. C 111 (2007) 13794–13803.
[32] N.T.T. An, D.Q. Dao, P.C. Nam, B.T. Huy, H.N. Tran, Surface enhanced Raman scattering of melamine on silver substrate: an experimental and DFT study, Spectrochimica Acta Part A: Mol. Biomol. Spectra 169 (2016) 230.
[33] B. Sharma, R.R. Frontiera, A.I. Henry, E. Ringe, R.P. Van Duyne, SERS: materials, applications, and the future, Mater. Today 15 (2012).
[34] M.J. Frisch, G.W. Trucks, H.B. Schlegel, G.E. Scuseria, M.A. Robb, J.R. Cheeseman, J.J.A. Montgomery, T. Vreven, K.N. Kudin, J.C. Burant, J.M. Millam, S.S. Iyengar, J. Tomasi, V. Barone, B. Mennucci, M. Cossi, G. Scalmani, N. Rega, G.A. Petersson, H. Nakatsuji, M. Hada, M. Ehara, K. Toyota, R. Fukuda, J. Hasegawa, M. Ishida, T. Nakajima, Y. Honda, O. Kitao, H. Nakai, M. Klene, X. Li, J.E. Knox, H.P. Hratchian, J.B. Cross, V. Bakken, C. Adamo, J. Jaramillo, R. Gomperts, R.E. Stratmann, O. Yazyev, A.J. Austin, R. Cammi, C. Pomelli, J.W. Ochterski, P.Y. Ayala, K. Morokuma, G.A. Voth, P. Salvador, J.J. Dannenberg, V.G. Zakrzewski, S. Dapprich, A.D. Daniels, M.C. Strain, O. Farkas, D.K. Malick, A.D. Rabuck, K. Raghavachari, J.B. Foresman, J.V. Ortiz, Q. Cui, A.G. Baboul, S. Clifford, J. Cioslowski, B.B. Stefanov, G. Liu, A. Liashenko, P. Piskorz, I. Komaromi, R.L. Martin, D.J. Fox, T. Keith, M.A. Al-Laham, C.Y. Peng, A. Nanayakkara, M. Challacombe, P.M.W. Gill, B. Johnson, W. Chen, M.W. Wong, C. Gonzalez, J.A. Pople Gaussian 09, Revision A.08 Inc., Wallingford, CT, 2009.
[35] Y. Zhao, D.G. Truhlar, The M06 suite of density functionals for main group thermochemistry, thermochemical kinetics, noncovalent interactions, excited states, and transition elements: two new functionals and systematic testing of four M06-class functionals and 12 other functionals, Theor. Chem. Acc. 120 (2008) 215.
[36] G.A. Petersson, A. Bennett, T.G. Tensfeldt, M.A. Al-Laham, W.A. Shirley, J.A. Mantzaris, A complete basis set model chemistry. I. The total energies of closed-shell atoms and hydrides of the first-row atoms, J. Chem. Phys. 89 (1988) 2193–2198.
[37] G.A. Petersson, M.A. Al-Laham, A complete basis set model chemistry. II. Open-shell systems and the total energies of the first-row atoms, J. Chem. Phys. 94 (1991) 6081–6090.
[38] A.D. McLean, G.S. Chandler, Contracted Gaussian-basis sets for molecular calculations. 1. 2nd row atoms, Z = 11–18, J. Chem. Phys. 72 (1980) 5639–5648.
[39] K. Raghavachari, J.S. Binkley, R. Seeger, J.A. Pople, Self-consistent molecular orbital methods. 20. Basis set for correlated wave-functions, J. Chem. Phys. 72 (1980) 650–654.
[40] P.J. Hay, W.R. Wadt, Ab initio effective core potentials for molecular calculations – potentials for the transition-metal atoms Sc to Hg, J. Chem. Phys. 82 (1985) 270–283.
[41] W.R. Wadt, P.J. Hay, Ab initio effective core potentials for molecular calculations – potentials for main group elements Na to Bi, J. Chem. Phys. 82 (1985) 284–298.
[42] P.J. Hay, W.R. Wadt, Ab initio effective core potentials for molecular calculations – potentials for K to Au including the outermost core orbitals, J. Chem. Phys. 82 (1985) 299–310.
[43] A.V. Marenich, C.J. Cramer, D.G. Truhlar, Universal solvation model base don solute electron density and on a continuum model of the solvent defined by the bulk dielectric constant and atomic surface tensions, J. Phys. Chem. B 113 (2009) 6378.

[44] A. Martínez, M.A. Rodríguez-Gironés, A. Barbosa, M. Costas, Donator acceptor map for carotenoids, melatonin and vitamins, J. Phys. Chem. A 112 (2008) 9037–9042.
[45] A. Martínez, R. Vargas, A. Galano, What is important to prevent oxidative stress? A theoretical study on Electron Transfer Reactions between carotenoids and free radicals, J. Phys. Chem. B 113 (2009) 12113–12120.
[46] T. Leisner, C. Rosche, S. Wolf, F. Granzer, L. Woste, The catalytic role of small coinage-metal clusters in photography, Surf. Rev. Lett. 3 (1996) 1105.
[47] R. Vargas, A. Martínez, Non-conventional hydrogen bonds: pterins-metal anions, Phys. Chem. Chem. Phys. 13 (2011) 12775–12784.
[48] A. Martínez, R. Vargas, Electron donor-acceptor properties of metal atoms interacting with pterins, New J. Chem. 34 (2010) 2988–2995.
[49] V. Bonačić-Koutecký, A. Kulesza, L. Gell, R. Mitrić, A.F. Bertorelle, R. Hamouda, D. Rayane, M. Broyer, T. Tabarin, P. Dugourd, Silver cluster–biomolecule hybrids: from basics towards sensors, Phys. Chem. Chem. Phys. 14 (2012) 9282–9290.
[50] A. Galano, R. Vargas, A. Martínez, Carotenoids can act as antioxidants by oxidizing the superoxide radical anion, Phys. Chem. Chem. Phys. 12 (2010) 193–200.